Thin Films as Superconductors Between Conventional Types I and II

W. Y. Córdoba-Camacho[1], R. M. da Silva[2], A. A. Shanenko[2,*], A. Vagov[3], A. S. Vasenko[1,4], B. G. Lvov[1], and J. Albino Aguiar[2]

[1]National Research University Higher School of Economics, Moscow, 101000, Russia
[2]Universidade Federal de Pernambuco, Departamento de Física, Recife, 50740-560, PE, Brazil
[3]Institut für Theoretische Physik III, Bayreuth Universität, Bayreuth, 95440, Germany
[4]I. E. Tamm Department of Theoretical Physics, P. N. Lebedev Physical Institute, Russian Academy of Sciences, 119991 Moscow, Russia
[*]arkadyshanenko@df.ufpe.br

ABSTRACT

Thin superconducting films are usually regarded as type-II superconductors even when they are made of a type-I materials. The reason is a strong influence of the stray magnetic fields outside the superconductive sample. While very thin films indeed reach this limit, there is a sufficiently large interval of film thicknesses in which the magnetic properties cannot be classified as either of the two conventional superconductivity types. We demonstrate that in this interval superconducting condensate and magnetic field reveal exotic spatial profiles that are very sensitive to system parameters, in particular, the temperature and applied field. Magnetic properties of such systems can be attributed to a special regime of intertype superconductivity. Its physical origin lies in the removal of infinite degeneracy of the superconducting state at the critical Bogomolnyi point. Here we demonstrate that qualitative characteristics of obtained condensate-field structures and the way they change with the temperature and applied field are independent of the choice of the in-plane boundary conditions for the order parameter and magnetic field.

Introduction

It has been demonstrated, both experimentally and theoretically, that the traditional dichotomic type I - type II classification of the superconductor magnetic properties is incomplete even in the simplest case of a clean BCS-like bulk superconductor[1–9] and has to be amended by a separate regime that can be referred to as the intertype (IT) superconductivity[10]. This regime is characterized by the non-standard magnetic response determined by exotic spatial condensate-field configurations. Its physical origin is general and intimately related to the critical Bogomolnyi point[11,12] at which the system becomes self-dual and all possible condensate-field configurations are degenerate. The IT superconductivity appears in the vicinity of the this point where the degeneracy is removed. The removal can take place due to a variety of reasons that, among others, include non-local interactions in the condensate below the critical temperature T_c (enhanced in the presence of many pairing channels due to multiple conduction bands[10]) and geometry related factors in finite and low-dimensional superconducting samples.

In particular, the IT regime can be found in sufficiently thin superconducting films where superconducting magnetic properties are modified by stray the magnetic fields outside the sample. It is well known that for sufficiently thin films made of a type-I material, stray fields result in repulsive interaction of vortices so that the magnetic response becomes that of type II[13–15]. This observation often leads to a tacit assumption that all sufficiently thin superconducting films are type-II superconductors. It has been recently demonstrated theoretically, however, that in a certain interval of the film thickness one should observe the magnetic response that is neither of the standard superconductivity types, which is similar to the phenomenon of the IT superconductivity in bulk[16]. Instead of lamellas, typical of type-I materials, or vortex lattices, expected in type-II superconductors, the films in the mentioned interval of thicknesses develop nonconventional condensate-field patterns such as condensate islands arranged in superstructures, vortex chains/labyrinths, and multiquantum (giant) vortices.

This analysis of the magnetic properties was done for infinitely large thin films[16], or to be more precise, for films with the artificial periodic boundary conditions. This choice of the boundary conditions raised questions on whether the obtained exotic intertype configurations can be artifacts of the periodic geometry. The point is that in real flat samples boundaries for the in-plane supercurrent (i.e., in-plane confinement boundary conditions) may influence the system via the interaction with the condensate state (e.g., the Bean-Livingston barrier[17]) as well as by modifying the magnetic field inside the sample. The corresponding modifications in the stray fields do not decay exponentially and are not negligible even at sufficiently large

distances from the in-plane boundaries. Moreover, a significant shortcoming of the periodic in-plane geometry is that due to the magnetic flux conservation, a perpendicular magnetic field penetrates the system at infinitely small absolute values, which is qualitatively different from the case of the in-plane confinement boundaries. It means that the transformation from the Meissner to the mixed state cannot be captured by the approach with the periodic in-plane boundaries. Last but not least is that in the vicinity of the Bogomolnyi point, where all condensate-field configurations in the mixed state are close to the degeneracy, changes in treatment of the boundaries can result in significant alterations of such configurations.

In this work we study details of the type I - type II crossover induced by the stray field in thin films made of a type-I material and with the in-plane confinement boundary conditions. The analysis is done by considering both the superconducting state inside and the stray field outside the sample. The goal of this work is to complement the previous study with the periodic geometry and investigate to what extent the choice of the in-plane boundary conditions affect the IT condensate-field configurations and qualitative features of the interchange between superconductivity types. The work demonstrates that the IT mixed state configurations in finite flat samples are qualitatively similar to those obtained in infinite films.

Results

The present study does not focus on mesoscopic samples, extensively considered previously, where superconducting vortices are directly restricted by the sample boundaries. On the contrary, thin superconductors considered in this work have dimensions that, except the thickness, exceed the vortex sizes considerably, as seen from the sketch in Fig. 1. Here in the presence of a perpendicular magnetic field, in-plane boundaries do not squeeze vortices, dictating bunching into unusual patterns, but affect the mixed state through the stray-field contribution controlled by the film thickness.

The obtained results are represented as temperature-dependent condensate configurations, calculated at several selected values of the film thickness at a fixed value of the external magnetic field [Fig. 2], and also as the field-dependent condensate patterns, calculated for a fixed temperature [Fig. 3].

0.1 Temperature dependence

Figure 2 demonstrates the spatial profile of the squared absolute value of the order parameter $|\Psi|^2$ (i.e., the condensate density) computed in the presence of the perpendicular external magnetic field $H = 0.1H_c(0)$ [$H_c(0)$ is the bulk thermodynamic critical magnetic field at $T = 0$] for different temperatures in the range $T = 0.6$-$0.78T_c$ and the film thicknesses $w = 2, 6$, and $8\xi_0$, with ξ_0 is the zero-temperature coherence length. One can see that for the thinnest film with $w = 2\xi_0$ the condensate configuration is typical for type II - the magnetic field penetrates the film in the form of separate vortices that carry a single quantum of the magnetic flux. Vortices are arranged in an almost periodic structure that is close to the triangular Abrikosov lattice (some disorder is present due to calculations). Close to the boundaries the superconductivity is enhanced which is typical for finite type-II superconductors placed in a non-zero magnetic field. The lattice distortions are more pronounced at higher temperatures due to slowing the numerical-procedure convergence near the point of the normal-to-superconducting transition. At this thickness the stray field makes a major contribution to the vortex-vortex interaction so that vortices, that attract each other in a type-I material, become repulsive and form a stable Abrikosov lattice in agreement with the well-known studies[13–15].

For thicker samples $w = 6$ and $8\xi_0$, the condensate spatial profile is dramatically different from what is expected for both conventional superconductivity types. Moreover the condensate patterns are very sensitive to temperature changes. At $T = 0.78T_c$ [Figs. 2 II(a) and III(a)] the field occupies almost all area of the sample with the exception of few islands of the superconducting condensate. Those islands form a lattice-like structure so that the situation is somewhat opposite to the Abrikosov lattices in type-II superconductors. At $T = 0.78T_c$ such a superstructure of superconductive islands is visible only for the thinner sample with $w = 6\xi_0$ [Fig. 2 II(a)] while for the thicker one with $w = 8\xi_0$ it develops at lower temperature $T = 0.75T_c$ [Fig. 2 III(b)]. One can see also vortices given by white empty circles in the blue background of an almost suppressed condensate.

When the temperature decreases further, the condensate profile for both widths $w = 6$ and $8\xi_0$ changes qualitatively. Both superconducting and non-superconducting regions expand into quasi-one dimensional structures. The latter arrange themselves in larger-scale patterns that tend to follow the symmetry of the sample [Figs. 2 II(b), II(c) and III(c)]. It is important that the regions with a strongly suppressed condensate are densely populated with vortices which are arranged in vortex chains that are most pronounced at $T = 0.7T_c$. Here one finds that the superstructures of the condensate islands are replaced by labyrinths of vortices that separate superconducting stripes.

For lower temperatures $T = 0.65$ and $0.6T_c$, the vortex chains break into smaller parts, eventually forming well separated vortices and vortex clusters. This takes place first in the middle of the sample whereas close to its boundaries vortices remain to be arranged in chains [Figs. 2 II(d), III(d) and III(e)]. At $T = 0.6T_c$ all vortex chains in the sample with $w = 6\xi_0$ are split into separate vortices and vortex clusters [Fig. 2 II(e)]. It should be noted that at this stage most of vortices are not single-quantum but carry several flux quanta (multiquantum vortices). Similar transformation can also be expected at lower temperatures for $w = 8\xi_0$. One can expect a similar trend for lower temperatures according to which multiquantum vortices and vortex clusters

finally become well separated single-quantum Abrikosov vortices arranged in a periodic lattice. However, as the use of the GL theory becomes questionable at sufficiently low temperatures, the corresponding results are avoided here.

0.2 Field dependence

The further insight into the behaviour of the condensate configurations can be obtained from their magnetic-field dependence. Results of the calculations are demonstrated in Fig. 3, where the spatial condensate distribution is given for the magnetic field in the range $H = 0.005\text{-}0.26H_c(0)$, as calculated at $w = 6\xi_0$ and $T = 0.6T_c$.

At $H = 0.005H_c(0)$ the sample develops the standard Meissner state [Fig. 3 (a)]. Here the field penetrates the sample only near the in-plane boundaries so that the condensate is suppressed close to the boundaries. When the field increases, it starts to penetrate the sample in the form of vortices appearing inside the sample [Fig. 3 (b)]. They carry a single quantum of the magnetic flux. From now on the Meissner state is replaced by the mixed state and the condensate density is no longer suppressed in the vicinity of the boundaries.

A further increase of the field gives rise to the appearance of multiquantum vortices [Fig. 3 (c)] and then to the formation of the vortex clusters [Fig. 3 (d)]. For larger magnetic fields vortex clusters expand and form vortex chains [Fig. 3 (d)]. Here the spatial profile of the condensate density becomes similar to that in Fig. 2 II(e). Vortex chains grow in length and eventually create symmetric structures that mirror the sample geometry [Fig. 3 (e)] and are similar to the patterns discussed above [c.f. Figs. 2 II(d) and II(c)]. For larger fields the regions of the suppressed order parameters expand and form domains of a nearly normal state that surround islands of the superconducting condensate [Figs. 3 (g) and (h)]. The obtained patterns are again similar to those in Fig. 2, see panels II(a) and III(b).

The appearance of multiquantum vortices can be easily seen from the corresponding spatial distribution of the condensate phase. An illustration is given in Fig. 4 which demonstrates the colour density plot of the phase (left panel) together with the corresponding condensate spatial distribution (right panel); the results are calculated at $T = 0.6T_c$ and $H = 0.08H_c(0)$ for $w = 6\xi_0$. In the phase plot one can see many examples when the phase changes its sign four times when moving around a vortex center. This means that the total phase span is 4π and the corresponding vortices carry two quanta of the magnetic flux.

One finds that the both Figs. 2 II, III and 3 demonstrate similar trends of the mixed-state transformation: at sufficiently low fields (with respect to the upper critical one) we observe Abrikosov vortices that, at higher fields, are converted into unconventional condensate-field patterns, including vortex clusters and multiquantum vortices, vortex chains/labyrinths, and finally the superstructures made of condensate islands.

Discussion

This work presents the study of the magnetic properties of thin superconductors with the in-plane confinement boundary conditions. The focus of the work is the crossover from type-I to type-II superconducting magnetic properties in films made of a type-I material.

The derived results demonstrate that within a certain range of the film thicknesses ($2\xi_0 \lesssim w \lesssim 10\xi_0$ for the material Ginzburg-Landau (GL) parameter $\kappa = 0.55$), the spatial condensate-field configurations in the mixed state differ considerably from those expected in types I and II. These configurations are found to be very sensitive to the system parameters. In particular, we have identified a general sequence of qualitative transformations in the condensate spatial distribution with the external field and temperature. Near the superconducting-to-normal transition, the condensate forms islands arranged in superstructures that reflect the sample geometry. These islands are surrounded by large domains with a significantly suppressed order parameter and vortices between neighbouring superconducting grains. When moving deeper into the mixed state, the nearly normal domains are transformed into closed-packed chains of vortices that separate superconducting islands while the latter become more elongated and form superconducting stripes. Then, starting from the inner part of the sample, the chains break into well separated vortices and vortex clusters. Such vortices can carry more than one quantum of the magnetic flux. Finally, when approaching the Meissner state, single-quantum vortices appear and tend to arrange themselves in an Abrikosov lattice.

The obtained condensate-field patterns and their transformations are similar to those calculated previously for thin superconductors with the in-plane periodic boundary conditions for the order parameter and magnetic field[16]. This proves that the qualitative picture of the mixed state in the IT superconducting films is not distorted by the in-plane periodic boundary conditions. However, the interaction with the fixed in-plane boundaries is noticeable and lead to arrangements of superstructures that mirror the sample geometry. We note, in passing, that the observed transformations of the condensate-field configurations are apparently more complex than what is suggested by the simplified type II/1 concept of the IT superconductivity[5]. This concept relies on the non-monotonic pairwise interaction between vortices with the long-range attraction. Here, the stray fields always result in the long-range repulsion, which makes the interaction qualitatively different. Furthermore, recent results for the IT domain in bulk samples suggests that it is many-body (many-vortex) interaction[18] that is responsible for the formation of vortex clusters and similar clusters are also calculated here for in thin films. We also remark that qualitatively similar mixed-state transformations have been observed in the recent study of superconducting nanowires in a perpendicular magnetic

field[19]. However, a direct comparison of the results for films and wires with those for bulk samples is not possible because a detailed investigation of the relevant field-condensate configurations in the mixed state of bulk IT superconductors is not completed yet.

Methods

Our analysis is done using the Ginzburg-Landau (GL) theory. It is known that the IT domain in bulk samples cannot be described within the GL approach as the GL equations predict a single singular point $\kappa_0 = 1/\sqrt{2}$ ($\kappa = \lambda/\xi$, λ is the magnetic penetration length, ξ is the GL coherence length) that separates type I ($\kappa < \kappa_0$) and type II ($\kappa > \kappa_0$) materials. In the GL theory the boundary between types I and II does not depend on the temperature and the IT regime is always restricted to a single point.

Corrections to the GL theory, which take into account non-local interactions in the condensate and which become important at temperatures $T < T_c$ (T_c is the superconducting transition temperature), removes the degeneracy and the critical point κ_0 unfolds into a finite interval or domain of the IT superconductivity. The single point (κ_0, T_c) in the κ-T plane, which separates superconductivity types at $T \to T_c$, remains infinitely degenerate and is referred to as the Bogomolnyi (critical) point.

However, the Bogomolnyi degeneracy can be also removed by other physical mechanisms, not related to the non-locality at lower temperatures. One of those is interactions of the condensate with sample boundaries and the stray field. Unlike the temperature-induced non-locality, those geometry-related mechanisms are captured within the GL approach. Consequently the GL theory can be used to describe the IT superconductivity for as long as those mechanisms prevail.

In the calculations we solve the GL equations, which are written in the dimensionless units[16] as

$$\begin{aligned} &\big(-i\nabla - \mathbf{A}\big)^2\Psi - (1-T)\big(1-|\Psi|^2\big)\Psi = 0, \\ &\kappa^2 \,\mathrm{rot}\,\mathbf{B} = (1-T)\,\mathbf{Re}\big[\Psi^*\big(-i\nabla - \mathbf{A}\big)^2\Psi\big], \end{aligned} \tag{1}$$

where Ψ is the condensate order parameter and $\mathbf{B} = \mathrm{rot}\,\mathbf{A}$ is the magnetic field. The zero-current boundary condition for the order parameter requires $\mathbf{n}\cdot\big(-i\nabla - \mathbf{A}\big)\Psi = 0$, which is to be fulfilled at the sample boundary, where $\mathbf{n}$ is the unit vector normal to the boundary In the present work this condition is also used for the in-plane supercurrent, which differs from the in-plane periodic boundary conditions for the order parameter and magnetic field in the previous study[16]. The field has to satisfy the asymptotic condition $\mathbf{B} = \mathbf{H}$ at infinity, where $\mathbf{H} = (0,0,H)$ is the applied magnetic field. In practical calculations we chose an outer surface at which this condition is satisfied - this has to be sufficiently far from the sample so that the choice does not influence the results. A sample is a slab with the thickness w and the two other dimensions L_a and L_b, with $L_a = 50\xi_0$ and $L_b = 75\xi_0$, where distances are given in units of the zero-temperature coherence length ξ_0. We choose $L_{a,b} \gg w$, as reflecting the film geometry, a sketch of the system is shown in Fig. 1, where the superconducting sample is marked by the red colour whereas the grey slab gives the outer surface where the asymptotic boundary condition for the magnetic field is invoked.

As usual, the GL equations (1) for Ψ and $\mathbf{B}$ are solved using the auxiliary time dependence method, where the equations for are amended with the first order time derivatives, such that the solution converges to the stationary one for sufficiently large times. The resulting time-dependent GL formalism is solved with the help of the link variable method[16,20].

The GL parameter of the film material is chosen to be $\kappa = 0.55$ which corresponds to type I. To illustrate how the superconducting magnetic response depends on the film thickness, we perform calculations for several chosen values of w in the interval $w \sim 2 - 8\xi_0$. We perform the numerical investigations down to $T \sim 0.6T_c$, where the GL theory is expected to apply at least qualitatively.

References

1. U. Krägeloh, Phys. Lett. A **28**, 657 (1969).
2. U. Essmann, Physica **55**, 83 (1971).
3. D. R. Aston, L. W. Dubeck, and F. Rothwarf, Phys. Rev. **3**, 2231 (1971).
4. A. E. Jacobs, Phys. Rev. B **4**, 3029 (1971).
5. J. Auer and H. Ullmaier, Phys. Rev. B **7**, 136 (1973).
6. U. Klein, J. Low Temp. Phys. **69**, 1 (1987).
7. H.W. Weber, E. Seidl, M. Botlo, C. Laa, E. Mayerhofer, F. M Sauerzopf, R.M. Schalk, and H.P. Wiesingerh, Physica C **161**, 272 (1989).
8. E. H. Brandt, Rep. Prog. Phys. **58**, 1465 (1995).
9. E. H. Brandt and M. P. Das, J. Supercond. Nov. Magn. **24**, 57 (2011).

10. A. Vagov, A. A. Shanenko, M.V. Milosevic, V. M. Axt, V. M. Vinokur, J. A. Aguiar, and F. M. Peeters, Phys. Rev. B **93**, 174503 (2016).

11. E. B. Bogomolnyi and A. I. Vainstein, Sov. J. Nucl. Phys. **23**, 588 (1976).

12. E. B. Bogomolnyi and A. I. Vainstein, Sov. J. Nucl. Phys. **24**, 449 (1976).

13. M. Tinkham, Phys. Rev. **129**, 2413 (1963).

14. J. Pearl, Appl. Phys. Lett. **5**, 65 (1964).

15. K. Maki, Ann. Phys. (NY) **34**, 363 (1965).

16. W.Y. Córdoba-Camacho, R.M. da Silva, A. Vagov, A. A. Shanenko, and J. A. Aguiar, Phys. Rev. B **94**, 054511 (2016).

17. C. P. Bean and J. D. Livingston, Phys. Rev. Lett. 12, 14(1964).

18. S. Wolf, A. Vagov, A. A. Shanenko, V. M. Axt, A. Perali, and J. A. Aguiar, Phys. Rev. B **95**, 094521 (2017).

19. W. Y. Córdoba-Camacho, R. M. da Silva, A. Vagov, A. A. Shanenko, and J. Albino Aguiar, Phys. Rev. B **98**, 174511 (2018).

20. R. Kato, Y. Enomoto, and S. Maekawa, Phys. Rev. B 47, 8016(1993).

Acknowledgements

This work was supported by the Brazilian agencies Coordenação de Aperfeiçoamento de Pessoal de Nível Superior (Grant No. 223038.003145/2011-00), Conselho Nacional de Ciência e Tecnologia (Grants No. 400510/2014-6 and No. 309374/2016-2), and FACEPE (APQ-0936-1.05/15). A.V. acknowledges support from the Russian Science Foundation under the Project 18-12-00429, which was used to study non-local interactions in superconductors. A. S. V. acknowledges support of the joint Russian-Greek Projects RFMEFI61717X0001 and T4ΔPΩ-00031 “Experimental and theoretical studies of physical properties of low-dimensional quantum nanoelectronic systems”.

Author contributions statement

A. Vagov, A. A. Shanenko and W. Y. Córdoba-Camacho were conceived of the idea; W. Y. Córdoba-Camacho and R. M. da Silva developed a numerical code and performed calculations; A. Vagov took the lead in writing the manuscript with support of A. A. Shanenko; J. Albino Aguiar, B. G. Lvov, and A. S. Vasenko contributed to the interpretation of results. All authors provided critical feedback and helped to shape the research and manuscript.

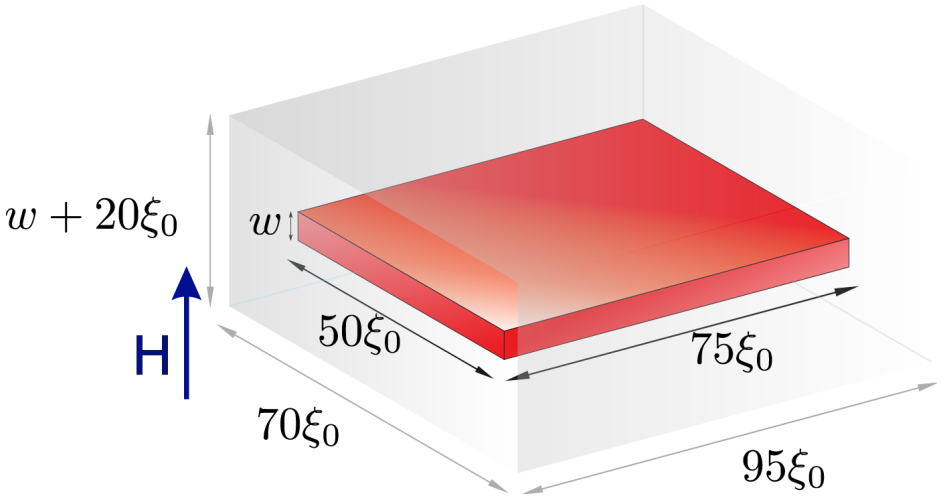

Figure 1. A sketch of the superconducting slab (red) placed in the external perpendicular uniform magnetic field **H**. In the grey area the field differs substantially from the uniform external magnetic field.

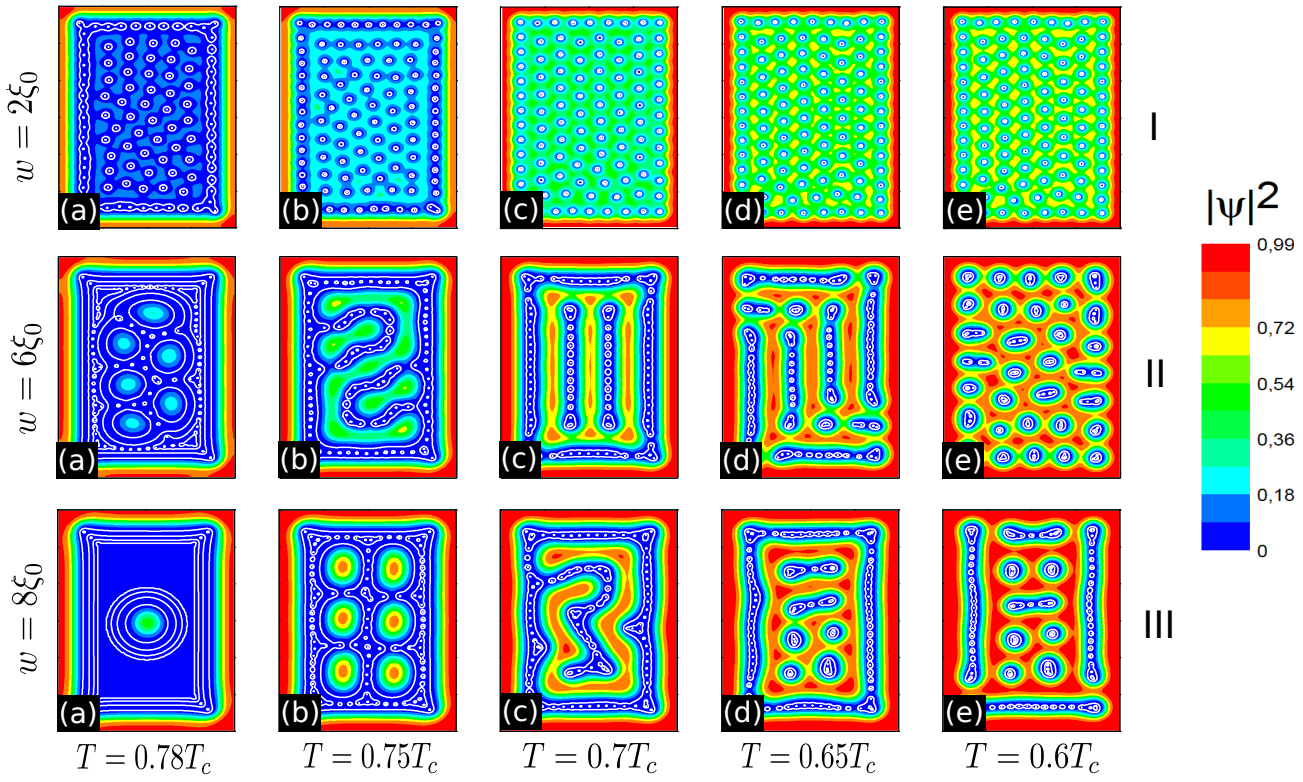

Figure 2. Color density plot of spatial configurations for the condensate density $|\Psi|^2$, calculated for different film thicknesses $w = 2\xi_0$ (upper row of panels - I), $w = 6\xi_0$ (middle row of panels - II), and $w = 8\xi_0$ (lower row of panels - III). Panels (a)-(e) are obtained at different temperatures, shown below the panels. The color scheme with the corresponding values is found on the right, the scaled density varies from $|\Psi|^2 = 1$ (full Meissner effect) to $|\Psi|^2 = 0$ (normal state). The calculations are done for external field $H = 0.1H_0(0)$.

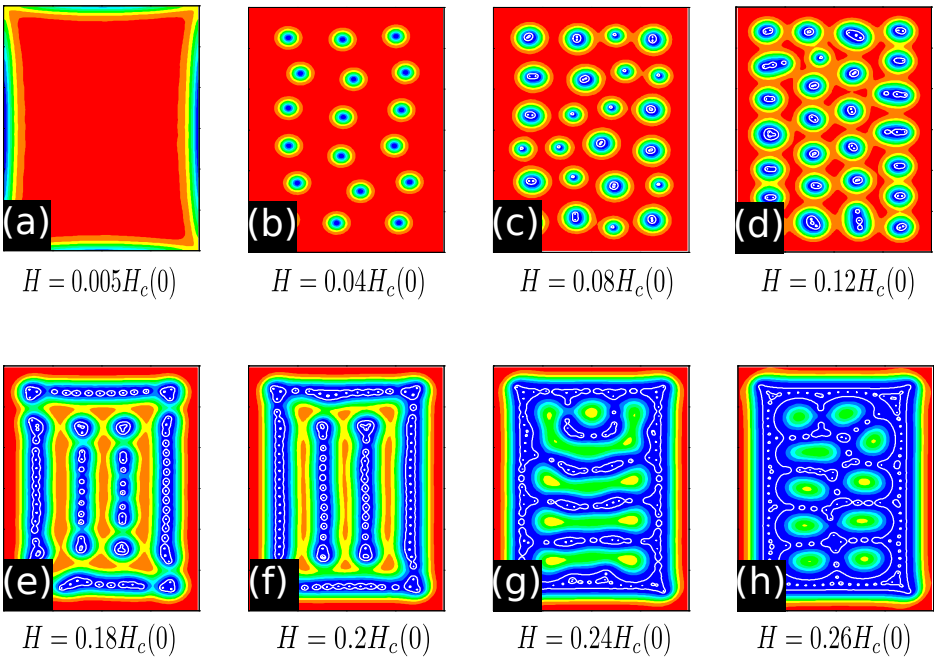

Figure 3. Panels (a)-(h) are color density plots of the condensate density $|\Psi|^2$, calculated for different values of the external magnetic field (shown below). Calculations are done at $T = 0.6T_c$ and for the film with thickness $w = 6\xi_0$.

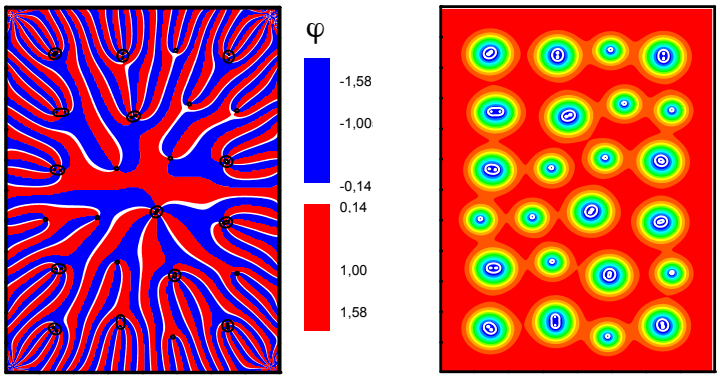

Figure 4. Phase portrait (left panel) corresponding to spatial profile of the condensate density (right panel), calculated at $T = 0.6T_c$ and $H = 0.1H_c(0)$. The colour scheme for the phase portrait is dichromic - blue for $\phi < 0$ and red for $\phi > 0$.